

# Higher-energy Collision Dissociation for the quantification by liquid chromatography-tandem ion trap mass spectrometry of nitric oxide metabolites coming from *S*-nitrosoglutathione in an *in vitro* model of intestinal barrier

Yu Haiyan<sup>1</sup>, Bonetti Justine<sup>1</sup>, Gaucher Caroline<sup>1</sup>, Fries Isabelle<sup>1</sup>, Vernex-Loiset Lionel<sup>2</sup>, Leroy Pierre<sup>1</sup>, Chaimbault Patrick<sup>2,\*</sup>

<sup>1</sup> Université de Lorraine, CITHEFOR, F-54000 Nancy, France

<sup>2</sup> Université de Lorraine, LCP-A2MC, F-57000 Metz, France

\* Correspondence to: Chaimbault Patrick, SRSMC UMR 7565, ICPM, 1 boulevard Arago, 57070 Metz, France

E-mail: [patrick.chaimbault@univ-lorraine.fr](mailto:patrick.chaimbault@univ-lorraine.fr)

## Abstract

**RATIONALE:** The potency of *S*-nitrosoglutathione (GSNO) as a nitric oxide (NO) donor to treat cardiovascular diseases (CVDs) has been highlighted in numerous studies. In order to study its bioavailability after oral administration, which represents the most convenient route for the chronic treatment of CVDs, it is essential to develop an analytical method permitting (i) the simultaneous measurement of GSNO metabolites, *i.e.* nitrite, *S*-nitrosothiols (RSNOs) and nitrate and (ii) them to be distinguished from other sources (endogenous synthesis and diet).

**METHODS:** Exogenous GSNO was labeled with <sup>15</sup>N, and the GS<sup>15</sup>NO metabolites after conversion to nitrite ion were derivatized with 2,3-diaminonaphthalene. The resulting 2,3-naphthotriazole was quantified by liquid chromatography-tandem ion trap mass spectrometry

This article has been accepted for publication and undergone full peer review but has not been through the copyediting, typesetting, pagination and proofreading process which may lead to differences between this version and the Version of Record. Please cite this article as doi: 10.1002/rcm.8287

(LC/ITMS/MS) in multiple reaction monitoring mode after Higher-energy Collision Dissociation (HCD). Finally, the validated method was applied to an *in vitro* model of intestinal barrier (monolayer of Caco-2 cells) to study GS<sup>15</sup>NO intestinal permeability.

**RESULTS:** A LC/ITMS/MS method based on an original transition ( $m/z$  171 to 156) for sodium <sup>15</sup>N-nitrite, GS<sup>15</sup>NO and sodium <sup>15</sup>N-nitrate measurements was validated, with recovery of  $100.8 \pm 3.8$ ,  $98.0 \pm 2.7$  and  $104.1 \pm 3.3$  %, respectively. Intra- and inter-day variabilities were below 13.4 and 12.6 %, and the limit of quantification reached 5 nM (signal over blank = 4). The permeability of labeled GS<sup>15</sup>NO (10-100  $\mu$ M) was evaluated by calculating its apparent permeability coefficient ( $P_{app}$ ).

**CONCLUSIONS:** A quantitative LC-ITMS/MS method using HCD was developed for the first time to selectively monitor GS<sup>15</sup>NO metabolites. The assay allowed evaluating GS<sup>15</sup>NO intestinal permeability and situated this drug candidate within the middle permeability class according to FDA guidelines. In addition, the present method has opened the perspective of a more fundamental work aiming at studying the fragmentation mechanism leading to the ion at  $m/z$  156 in HCD tandem mass spectrometry in the presence of acetonitrile.

**Key words:** <sup>15</sup>N-nitrite, <sup>15</sup>N-nitrate, <sup>15</sup>N-S-nitrosoglutathione, 2,3-diaminonaphthalene, LC-ITMS/MS

## INTRODUCTION

Nitric oxide (NO) is a gaseous messenger playing an important role in the vascular system homeostasis<sup>1</sup>. Its origin includes both endogenous (catabolism of arginine catalyzed by endothelial NO synthase)<sup>2,3</sup> and exogenous (intake of drinking water and food)<sup>4</sup> sources. The endogenous production of NO decreases with ageing<sup>5</sup> and cardiovascular diseases (CVDs) related to endothelial dysfunction. In this case, an exogenous supply of NO is necessary. Currently, drugs used as NO donors have major drawbacks such as oxidative stress induction and tolerance phenomenon<sup>6,7</sup>. Many studies highlight the potency of *S*-nitrosothiols (RSNOs) as NO donors, especially *S*-nitrosoglutathione (GSNO)<sup>8</sup>, because they do not exhibit the side effects previously cited<sup>9</sup>. However, very few reports have been focused on their bioavailability after oral administration<sup>10</sup>, which is their most convenient route for the chronic treatment of CVDs. Then small intestine is the major barrier for the efficient absorption of orally administered therapeutics<sup>11,12</sup>. Caco-2 trans-epithelial permeability assay (monolayer of differentiated Caco-2 cells) is the *in vitro* model commonly used for intestinal absorption studies of drugs<sup>13,14</sup>. Thus, using this model is the first step to evaluate the intestinal permeability of GSNO and its bioavailability.

In a biological environment, GSNO is easily decomposed by metal ions, reductants, enzymes or light, resulting in a release of NO<sup>9</sup>. This reactive species is then rapidly oxidized into nitrite and nitrate ions<sup>4</sup>. Moreover, GSNO undergoes a transnitrosation process corresponding to NO moieties exchange with a cysteine residue of peptides and proteins, resulting in a formation of RSNOs<sup>8</sup>. The different GSNO metabolites, *i.e.* nitrite, nitrate ions and RSNOs, represent a NO reservoir<sup>9</sup>. *S*-nitrosation of proteins is also a post-translational pathway playing a key role in many physiopathological processes<sup>8,9,15</sup>. GSNO metabolites should be measured together because they give complementary information<sup>4,8,9</sup>. Thus, there is a great need to develop appropriate assays in this field. Actually, very few assays allow the determination of all cited NO species in the same methods<sup>16,17,18</sup>.

Mass spectrometry is a widespread technique used for the quantification of metabolites of interest in biological samples because of its high specificity of detection (multiple reaction

monitoring (MRM) mode) and its sensitivity for trace level measurement. Because of its low molecular mass, NO (30 u) has to be derivatized to allow its measurement in cells or biological fluids (urine, plasma, etc). Indeed, it is not possible for many commercially available mass spectrometers to reach such a low  $m/z$  value and the background noise is usually high at low masses. As mentioned above, NO is rapidly converted into nitrite and nitrate ions, which are the real derivatized compounds. For pharmacology studies, there is a need to quantify NO species coming from administered NO donor drugs regardless of whether they come from endogenous synthesis or diet intake. Mass spectrometry allows distinguishing NO species coming from administered NO donors and those from endogenous synthesis and diet intake, thanks to the incorporation of the stable nitrogen isotope  $^{15}\text{N}$  into the NO donor (presently  $\text{GS}^{15}\text{NO}$ ). Indeed, the  $^{15}\text{N}$  isotope is stable and its natural abundance level represents 0.37% of all nitrogen isotopes<sup>19</sup>. Thus, it is possible to monitor specifically adducts labeled either with  $^{14}\text{N}$  (corresponding to the endogenous production and the diet uptake) or with  $^{15}\text{N}$  (corresponding to the drug uptake).

In addition to the increase in molecular mass, the derivatization procedure facilitates nitrite and nitrate ions analysis either by gas chromatography (the nitrite ion is transformed into a volatile derivative) or by Reversed Phase Liquid Chromatography (nitrite ion is transformed into a more hydrophobic derivative increasing the retention on this kind of stationary phases). The GC-CI-MS method developed by Tsikas *et al* uses pentafluorobenzyl bromide (PFBBBr) for  $^{15}\text{N}$ -nitrite and  $^{15}\text{N}$ -nitrate derivatization. It has the benefit of measuring derivatized nitrite and nitrate ions in the same chromatographic run<sup>20</sup>. The method in liquid chromatography-tandem mass spectrometry (LC-MS/MS) reported by Hanff and coworkers uses reduced *L*-glutathione (GSH) for  $^{15}\text{N}$ -nitrite derivatization and simultaneously analyzes nitrite ion and  $\text{GSNO}^{21}$ . This assay relies upon the *S*-nitrosation reaction between GSH as a probe and the nitrite ion to yield GSNO. 2,3-diaminonaphthalene (DAN) is a fluorogenic probe which reacts with nitrite ion to yield 2,3-naphthotriazole (NAT) adduct<sup>22</sup> (Figure 1A). It has been widely used with spectrofluorimetric direct detection<sup>23</sup> or coupled with LC<sup>22</sup> and even LC-MS/MS associated with  $^{15}\text{N}$ -nitrite derivatization and  $^{15}\text{N}$ -nitrate after reduction *via*

enzymatic catalysis<sup>24,25,26</sup> (Figure 1C). Currently, there is no report of using LC-MS/MS to measure RSNOs after DAN derivatization. For RSNOs, mercuric ions are commonly used to cleave the S-NO bond with further analysis of released nitrite ion<sup>27</sup> (Figure 1B).

This paper presents the development of a DAN-based LC-MS/MS assay for selectively monitoring all NO species metabolized from <sup>15</sup>N-labeled GSNO (nitrite, nitrate ions and RSNOs). For the first time, all these NO species will be quantified using the same analytical approach, providing a significant contribution to understanding the mechanism of GSNO metabolism. Currently, the publications related to a DAN-based LC-MS/MS assay<sup>24,25,26</sup> involve either a triple quadrupole mass spectrometer or a Q-trap instrument (operated as a triple quadrupole). This is easily understandable as triple quadrupole apparatus are well known to be the most sensitive tandem mass spectrometers for quantification when they are operated in MRM mode. However, this kind of spectrometer is not always available in the laboratory, and here we evaluated the sensitivity of Ion Trap Mass Spectrometry (ITMS) for the quantification of NO traces associated to the potential benefit of the Higher-energy Collision Dissociation (HCD) mode in this field. This original fragmentation method which cannot be used with a triple quadrupole mass spectrometer was compared with the traditional Collisionally Induced Dissociation (CID) available on both Ion trap and triple quadrupole mass spectrometers. Thus, the presented method involves liquid chromatography coupled to tandem ion trap mass spectrometry (LC-ITMS/MS) for the selective quantification of NO species metabolized from GS<sup>15</sup>NO. DAN will be used for the derivatization of free <sup>15</sup>N-nitrites and <sup>15</sup>N-nitrites coming from <sup>15</sup>N-nitrates and RS<sup>15</sup>NO species. The resulting adduct will be further analyzed by LC-ITMS/MS. Finally, the method will be validated and applied to study the intestinal permeability of GS<sup>15</sup>NO with use of an *in vitro* model.

## EXPERIMENTAL

### Chemicals and reagents

All reagents and standards are analytical grade and used without further purification. DAN, GSH, sodium  $^{15}\text{N}$ -nitrate ( $\text{Na}^{15}\text{NO}_3$ ), 2-naphthylamine (2-NA) and mercuric chloride ( $\text{HgCl}_2$ ) were obtained from Sigma-Aldrich (Saint-Quentin-Fallavier, France); sodium  $^{15}\text{N}$ -nitrite ( $\text{Na}^{15}\text{NO}_2$ ) was from Cambridge Isotope Laboratories (Tewksbury, MA, USA) and  $^{14}\text{N}$ -NAT from Chemodex (St. Gallen, Switzerland). Ultrapure deionized water ( $> 18.2 \text{ M}\Omega \cdot \text{cm}$ ) was used for the preparation of all solutions.

### S-nitrosoglutathione ( $\text{GS}^{15}\text{NO}$ ) synthesis

$\text{GS}^{15}\text{NO}$  was synthesized as already described<sup>28</sup> for  $\text{GS}^{14}\text{NO}$ : 20 mM GSH was incubated with 20 mM  $\text{Na}^{15}\text{NO}_2$  in 500 mM HCl at  $4^\circ\text{C}$  in the dark for 1 h. The reaction was stopped by neutralization with NaOH (40%) and the reaction mixture was further two-fold diluted with 500 mM phosphate buffer, pH 7.4. The final concentration was determined by UV spectrophotometry at a wavelength of 334 nm ( $\epsilon = 922 \text{ L} \cdot \text{mol}^{-1} \cdot \text{cm}^{-1}$ ).

### 2,3-Diaminonaphthalene (DAN) derivatization

The strategy of analysis using the same LC-ITMS/MS approach after DAN derivation of the different  $\text{GS}^{15}\text{NO}$  metabolites ( $^{15}\text{N}$ -nitrites,  $^{15}\text{N}$ -nitrates and  $\text{RS}^{15}\text{NO}$ ) generated during the *in vitro* study is depicted in Figure 2.

$^{15}\text{N}$ -nitrite standard solutions were prepared daily in Hank's Balanced Salt Solution (HBSS; NaCl, KCl, glucose,  $\text{KH}_2\text{PO}_4$ ,  $\text{Na}_2\text{HPO}_4$ ,  $\text{CaCl}_2$ ,  $\text{MgSO}_4$ , pH 7.4). Three hundred  $\mu\text{L}$  of standard solutions were mixed with 60  $\mu\text{L}$  of 0.105 mM DAN in 0.6 M HCl, incubated at  $37^\circ\text{C}$  for 10 min (Figure 1A). The addition of 36  $\mu\text{L}$  of 1 M NaOH and 4  $\mu\text{L}$  of 0.1 mM NaOH stopped the reaction. The real samples were similarly treated and their analysis provided the concentration of free  $^{15}\text{N}$ -nitrites in the *in vitro* model (⊙).

$^{15}\text{N}$ -nitrate was enzymatically converted into  $^{15}\text{N}$ -nitrite by using Nitrate/Nitrite Fluorometric Assay Kit (Cayman Chemical, Ann Arbor, MI, USA) with some modifications (Figure 1C). Briefly, 40  $\mu\text{L}$  of  $^{15}\text{N}$ -nitrate standard solutions were diluted with 120  $\mu\text{L}$  of assay buffer (Item N0. 780022). The resulting mixture was incubated at room temperature for

60 min after adding 20  $\mu\text{L}$  of enzyme cofactor (Item NO. 780012) and 20  $\mu\text{L}$  of nitrate reductase (Item NO. 780010). To continue the derivatization reaction, the mixture was immediately processed as described for the nitrite ion by adding 40  $\mu\text{L}$  of 0.105 mM DAN and incubating at 37°C for 10 min, followed by the addition of 24  $\mu\text{L}$  of 1 M NaOH and 3  $\mu\text{L}$  of 0.1 mM NaOH. The real samples were similarly treated and their analysis provided the cumulative concentration of free  $^{15}\text{N}$ -nitrites and  $^{15}\text{N}$ -nitrates (②) in the *in vitro* model. The  $^{15}\text{N}$ -nitrate concentration in the *in vivo* model (③) was then obtained by subtracting the concentration of free nitrites (③=②-①).

The quantification of  $\text{RS}^{15}\text{NO}$ s is carried out using a calibration curve built with  $\text{GS}^{15}\text{NO}$  in presence of mercuric ions: 300  $\mu\text{L}$  of  $\text{GS}^{15}\text{NO}$  standard solution were incubated with 60  $\mu\text{L}$  of 0.105mM DAN solution containing 1.05 mM  $\text{HgCl}_2$  in 0.6 M HCl at 37 °C for 10 min. The addition of 36  $\mu\text{L}$  of 1 M NaOH and 4  $\mu\text{L}$  of 0.1 mM NaOH stopped the reaction. The real samples were similarly treated to provide the cumulative concentration of free  $^{15}\text{N}$ -nitrites and  $\text{RS}^{15}\text{NO}$  (④) in the *in vitro* model. The  $\text{RS}^{15}\text{NO}$  concentration in the *in vivo* model (⑤) was then obtained by subtracting the concentration of free nitrites (⑤=④-①).

All resulting solutions were frozen at  $-80\text{ }^\circ\text{C}$  for a maximum period of 3 months, until analysis by LC-ITMS/MS.

2-Naphthylamine (2-NA) was used as internal standard (IS). For quantitative analysis, each sample was spiked with 10  $\mu\text{L}$  of a 0.02 mM solution of 2-NA prepared in acetonitrile-water (50/50, v/v).

### **Analysis of 2,3-naphthotriazole (NAT) by LC-ITMS/MS**

A Dionex Ultimate 3000 liquid chromatograph (Dionex, Sunnyvale, CA, USA) was coupled with an ion trap mass spectrometer (LTQ Velos Pro, Thermo Scientific, San Jose, CA, USA) fitted with the HESI-II probe (electrospray) operated in positive ion mode. Data were collected and analyzed with Tune Plus software (Thermo Scientific). The injection volume was 20  $\mu\text{L}$ . The separation was carried out on a Thermo Scientific Extend-C18 (2.1  $\times$  150 mm ID, 3  $\mu\text{m}$ ) column at a temperature of 25 °C. The mobile phase was composed of A: 0.01 M acetic acid and B: acetonitrile, delivered at 200  $\mu\text{L}\cdot\text{min}^{-1}$  in a gradient mode. The

column was first equilibrated at 40% B. When the sample was injected, the percentage of B increased to 80% over 3.5 min and held for 2.5 min. The column was re-equilibrated for 10 min between two sample runs. In these chromatographic conditions, NAT is eluted from the column in 5.5 min and 2-NA in 6.6 min (Figure 3). In addition, during the first 3 min, the mobile phase was directed to waste using a switching valve in order to limit the contamination of the mass spectrometer by the matrix.

The electrospray voltage was +5.0 kV. The ion source and capillary temperatures were 280 and 250 °C, respectively. The sheath, auxiliary and sweep gas flows were set at 10, 5 and 0 (arbitrary units) respectively. For quantification, the best MS/MS conditions were reached by optimizing the collision energy for each analyte in order to obtain the highest signal. The selected reaction monitoring (SRM) method recorded the following transitions for the analytes:  $m/z$  171 to 156 for  $^{15}\text{N-NAT}$  or  $m/z$  170 to 156 for  $^{14}\text{N-NAT}$  via their respective acetonitrile adduct ( $m/z$  212 and 211) formed in HCD cell (the formation of the adduct with this acetonitrile and the choice of these transitions will be discussed later on in the result and discussion section) obtained in HDC at 50 eV and  $m/z$  144  $\rightarrow$  117 for the IS (2-NA) in CID at 35 eV. The activation Q value was 0.250 and the isolation window was 1u for each transition.

Samples were randomized to prevent batch effect, paired and run in sequence.

### **Method validation and quality control**

A six-point calibration curve (blank, 5, 10, 20, 50, 100, 200 nM) for  $\text{Na}^{15}\text{NO}_2$  and  $\text{GS}^{15}\text{NO}$ , and a five-point calibration curve (blank, 250, 500, 1250, 2500, 5000 nM) for  $\text{Na}^{15}\text{NO}_3$  were made in HBSS. They were used to calculate the limits of quantification (LOQ), to check the linear range and to determine the percentage of recovery. Background levels of  $^{15}\text{N}$ -nitrite,  $\text{GS}^{15}\text{NO}$  and  $^{15}\text{N}$ -nitrate in HBSS corresponding to blanks were measured and subtracted from all quantification values. Three concentrations (15, 50 and 180 nM) of  $\text{Na}^{15}\text{NO}_2$  and  $\text{GS}^{15}\text{NO}$  and (300, 2500 and 4000 nM) of  $\text{Na}^{15}\text{NO}_3$  in HBSS were analyzed six times to determine the intra-day precision and accuracy. The number of replicates for the inter-day validation was also six. The inter-day statistics were determined from three independent analytical runs, each containing the calibration standards and two QC samples at

low, medium and high concentration levels. A six-point calibration curve of Na<sup>15</sup>NO<sub>2</sub> in HBSS was daily run to assess instrument performances.

### **Permeability studies of GS<sup>15</sup>NO on Caco-2 cell monolayer model**

The permeability of GS<sup>15</sup>NO across the Caco-2 monolayer was evaluated in the apical-to-basolateral direction in HBSS buffer containing Ca<sup>2+</sup> and Mg<sup>2+</sup> as previously described<sup>10</sup>. Briefly, 2×10<sup>6</sup> cells·cm<sup>-2</sup> were seeded on cell culture inserts (Transwell®, Corning, NY, USA) with 0.4 μm pore size disposed in a 12-wells plate. The medium was replaced every two days during the first week and daily during the final days, until the differentiated cell monolayer was formed (14-18 days, transepithelial electrical resistance (TEER) > 500 Ω·cm<sup>-2</sup>). TEER was measured with a Millicell®-Electrical Resistance System (Millipore, Billerica, MA, USA).

For permeation experiments, 500 μL of HBSS containing 10, 25, 50 or 100 μM of GS<sup>15</sup>NO were introduced into the apical (donor) compartment. The basolateral (receptor) compartment was filled with 1.5 mL of HBSS. After 1 h of permeation at 37°C, both compartments were harvested and diluted with HBSS to fit the ranges of calibration curves for <sup>15</sup>N-nitrite, GS<sup>15</sup>NO and <sup>15</sup>N-nitrate analysis. The resulting dilutions were immediately derivatized with DAN and stored at -80 °C until analysis by LC/ITMS/MS. After each permeation study, the integrity of the Caco-2 cell monolayer was evaluated by TEER measurement and sodium fluorescein (5 μM) permeability assessment.

The cumulative amounts of GS<sup>15</sup>NO permeated through the Caco-2 cell-monolayer were calculated from the concentrations measured in the basolateral compartment. The apparent permeability coefficient (P<sub>app</sub>) values were calculated using the following equation:

$$P_{app} = \frac{dQ}{dt} \times \frac{1}{A \times C_0}$$

dQ/dt (mol·s<sup>-1</sup>) refers to the quantity of permeated <sup>15</sup>NO species (dQ) in the basolateral compartment at the time of quantification (dt), A refers to membrane diffusion area (1.12 cm<sup>2</sup>), and C<sub>0</sub> refers to the initial concentration of GS<sup>15</sup>NO in the apical compartment (from 1.10<sup>-5</sup> to 1.10<sup>-4</sup> M).

For each concentration level evaluated (incubation with 10, 25, 50 and 100  $\mu\text{M}$  of GS<sup>15</sup>NO), the permeation experiments were carried out 3 times.

### Statistical analysis

All results are expressed as the means  $\pm$  standard deviation. The Student's t-test was used to determine significant differences ( $p < 0.05$ ).

## RESULTS AND DISCUSSION

Nitric oxide is very unstable and turns rapidly into nitrite ion ( $\text{NO}_2^-$ ) which is the real measured compound. In the field of LC, nitrites are often derivatized by the 2,3-diaminonaphthalene (DAN). The resulting 2,3-naphthotriazole (NAT) derivative allows its detection by fluorescence (Figure 1). The DAN-based fluorescence LC method is particularly appreciated for the analysis of nitrites (and nitrates after enzymatic reduction) in all biological samples because of its simplicity of use, the rapidity of the sample preparation, and the easy automation<sup>29</sup>. However, the fluorescence detection does not allow the distinction of isotope labeling and the quantification of NO metabolites in the nM range (LOD is around 100 nM with DAN-based fluorescence HPLC).

Currently, there are only three publications related to DAN-based LC-MS/MS assays found in the literature<sup>24,25,26</sup>. All these experiments were carried out either with a triple quadrupole or with a Q-trap instrument using the CID fragmentation mode. In 2011, Shin *et al.*<sup>26</sup> reached a LOQ of 4nM and their method was only validated for the measurement of  $\text{NO}_2^-$ . In 2016, Chao *et al.*<sup>24</sup> published the quantification by DAN-based LC-MS/MS in urine of  $\text{NO}_2^-$  and of  $\text{NO}_3^-$  after on-line solid phase extraction. For the first time, the interference on the <sup>15</sup>N-labeled NAT due to the natural presence of <sup>13</sup>C is evoked and estimated to be 2.2% (in good agreement with the theoretical value) of the contribution of the followed transition for this derivative. The same year, Axton *et al.*<sup>25</sup> reached a LOQ of 1nM in water and in the Dulbecco's Modified Eagle Medium (DMEM). However, the values of interferences of in the blank samples were not discussed whereas they were 91 and 339 nM for <sup>14</sup>N-nitrites in water and DMEM respectively. Thus, the interference due to <sup>13</sup>C on the signal <sup>15</sup>N-nitrite signal in

the blank samples should be around 2 nM in water and 7.5 nM in DMEM. These interference levels have to be considered to appreciate the LOQ in the real samples.

In this paper, we evaluated the sensitivity of an Ion Trap Mass Spectrometer associated to the Higher-energy Collision Dissociation mode for the quantification of NO metabolite traces. To achieve this goal, we compared the performance of the HCD mode with the CID mode traditionally used and the blank values were also discussed to provide the LOQ in the real samples. The method developed and validated in this paper was also tested to monitor NO freed from RSNOs.

### **Optimization of the LC-ITMS/MS detection - Comparison between CID and HCD**

The NAT adduct resulting from the derivatization of nitrite ion with DAN was quantified by LC/ITMS/MS. Its quantification at trace level supposed the optimization of the whole analytical pathway. Among the existing literature on NAT analysis by reversed phase LC/MS/MS, acetonitrile (ACN) and methanol (MeOH) have been used as organic modifiers in the mobile phase in combination with various acidic buffers. In our study, the most intense MS signal was obtained with a 10 mM acetic acid solution combined with ACN in gradient elution (see experimental section for details). Acetonitrile improved the sensitivity of NAT detection by a factor of 10 compared with MeOH. The analysis took 7 min with a re-equilibration time of 10 min between two injections. The gradient helped to reduce peak widths and thus improved the sensitivity.

Acetonitrile also showed another interesting effect when we compared the two modes of fragmentation with the LTQ Velos Pro ion trap instrument: the commonly used Collisionally Induced Dissociation and Higher-energy Collision Dissociation. The CID mode led to the same fragmentation pathway already published when using a triple quadrupole instrument<sup>24,25,26</sup> (Figure 4A). The protonated <sup>14</sup>N-NAT (*m/z* 170) yielded two product ions at *m/z* 142 (loss of N<sub>2</sub>) and *m/z* 115 (the indene ion [C<sub>9</sub>H<sub>7</sub>]<sup>+</sup> derived from *m/z* 142 and comprising the rest of the naphthyl ring after the loss of HCN)<sup>25</sup>.

The fragmentation in HCD was slightly different from that in CID (Figure 4B). When  $m/z$  170 is isolated and MS/MS experiments are carried out on this ion, the ultimate product ion at  $m/z$  115 remained the same but the intermediate product ion was now observed at  $m/z$  156. There is thus a difference of 14 u between this product ion and its precursor ion. This difference, which cannot obviously be assigned to a loss of a single nitrogen atom (N) or a methylene group ( $\text{CH}_2$ ), has another complex origin which has been resolved through several complementary experiments detailed below (Figures 4C and 4D, and Table 1):

- When MeOH replaced ACN in the mobile phase, the CID and HCD spectra showed the same transition. In both cases, the precursor ion  $[\text{}^{14}\text{N-NAT+H}]^+$  produced two transitions  $m/z$  170  $\rightarrow$  142 and  $m/z$  170  $\rightarrow$  115. Thus, the presence of ACN is responsible of the original fragment at  $m/z$  156.
- In this work,  $^{15}\text{N-NAT}$  is quantified in order to monitor NO coming from the parent drug. Its corresponding HCD MS/MS spectrum is provided in Figure 4D. The precursor ion  $[\text{}^{15}\text{N-NAT+H}]^+$  at  $m/z$  171 produced two fragments at  $m/z$  156 and 115. The observed fragments are the same as for  $[\text{}^{14}\text{N-NAT+H}]^+$ . The conclusion is that  $^{15}\text{N}$  is lost during the fragmentation from  $m/z$  171 to 156.
- In order to understand what happened in the HCD cell with ACN during the fragmentation, the  $^{14}\text{N}$ - and  $^{15}\text{N}$ -labeled NAT were infused using the LC mobile phase containing either ACN or  $\text{d}_3\text{-ACN}$ . The results are displayed in Table 1, and Figures 4C and 4D. The hypothesis was the formation of a  $[\text{NAT+H+ACN}]^+$  adduct, confirmed by the presence of a peak at  $m/z$  211 for  $^{14}\text{N-NAT}$  in ACN and  $m/z$  214 in  $\text{d}_3\text{-ACN}$ . This adduct underwent a rearrangement during fragmentation leading to  $m/z$  183 by  $\text{N}_2$  loss ( $m/z$  186 with  $\text{d}_3\text{-ACN}$ ). Then, an additional HCN loss led to  $m/z$  156 from  $m/z$  183 or  $m/z$  159 from  $m/z$  186 with  $\text{d}_3\text{-ACN}$ . All these ions were perfectly visible on the mass spectra (even if some of them exhibited a very low intensity). The values of  $m/z$  observed for each ion were consistent with this explanation whatever the derivative ( $^{14}\text{N}$  or  $^{15}\text{N-NAT}$ ) and the solvent condition (ACN or  $\text{d}_3\text{-ACN}$ ), as illustrated in Table 1 and Figure 4. From these last experiments, we concluded that ACN probably strongly interacted with the  $[\text{NAT+H}]^+$  ion

in the HCD cell. This is probably due to the specific position of the HCD cell in the LTQ Velos Pro mass spectrometer (see supplementary data, Figure S1), which is located upstream of the CID trap. In this particular design, the parent ion is first isolated in the linear iontrap then ejected back to the  $Q_{00}$  region where its fragmentation occurs. Then, the generated fragments are directed toward the linear iontrap where they are analyzed. In this process, it is easy to understand that the solvent vapors can enter the HCD cell making possible the reaction between  $[\text{NAT}+\text{H}]^+$  and ACN to produce this original fragmentation pathway. The fragmentation pathway can be summarized as follows ( $[\text{}^{14}\text{N-NAT}+\text{H}]^+$  is taken as example):

❖ In CID,  $m/z$  170 losses  $\text{N}_2$  to give  $m/z$  142 which in turn loses HCN to give  $m/z$  115.

This pathway was checked by  $\text{MS}^3$  which allows the observation of the transition  $m/z$  142  $\rightarrow$  115.

❖ In HCD,  $m/z$  170 reacts or interacts with ACN to give  $m/z$  211 ( $[\text{}^{14}\text{N-NAT}+\text{H}+\text{ACN}]^+$ ).

Then  $m/z$  211 undergoes two consecutive fragmentations, one loss of  $\text{N}_2$  ( $m/z$  183) and one loss of HCN, to give the original  $m/z$  156. Unfortunately, the signal intensities of  $m/z$  211 and 183 are too weak to check this pathway by  $\text{MS}^3$  but interestingly, these neutral losses are precisely the same (and in the same order) as observed from  $m/z$  170 in CID. The last step consists in the loss of the solvent molecule from  $m/z$  156 to restore  $m/z$  115 also observed in CID. This final pathway was checked by an  $\text{MS}^3$  experiment in CID at 35 eV, which allows the observation of the transition  $m/z$  156  $\rightarrow$  115. The ion  $m/z$  156 can be somehow described as the ACN adduct of  $m/z$  115  $[\text{C}_9\text{H}_7+\text{ACN}]^+$ , then  $m/z$  183 is corresponding to the ACN adduct of  $m/z$  142 (in CID) but the precursor of these fragment ion  $m/z$  211 ( $[\text{}^{14}\text{N-NAT}+\text{H}+\text{ACN}]^+$ ) is not observed in the source (see supplementary data, Figure S2) meaning that the ACN adduct is only formed thanks to the HCD process.

The reaction mechanism remains unclear at this time and its elucidation would deserve future investigation but the combination of ACN in the mobile phase and the HCD mode allowed us to reach a limit of quantification of 1 nM for the NAT adduct, by following the

new “indirect” SRM transition (i.e.  $m/z$  171 to 156 for  $^{15}\text{N}$ -NAT via the acetonitrile adduct  $m/z$  212 formation in the HCD cell). For the transition  $m/z$  171 to 115, the LOQ was 10 nM in HCD mode and only 20 nM in CID (best achievable results in CID). This value was within the same range as in previous studies for the measurement of  $^{15}\text{N}$ -nitrite by LC-MS/MS<sup>25,26</sup>. The chosen transitions for each compound (including the IS, i.e. the 2-naphthylamine) are reported in the experimental section. The method was then validated to monitor with accuracy the NO species freed from GSNO in an *in vitro* model of intestinal barrier at trace levels.

### **Interferences in blank samples and working LOQ**

The final objective of this study is to assess the permeability of GSNO across the intestinal barrier by means of an *in vitro* model (Caco-2 monolayer). During the incubation, Caco-2 cells secreted many metabolites into the buffer, including unlabeled NO species. Thus, the incubation medium turned into a complex biological matrix, which required a high specific or selective method of analysis. In this field, LC-MS/MS has become the standard technique, being much more specific, selective and even much more sensitive than most other conventional spectroscopic techniques (UV and even fluorescence). The selectivity has been tested by analyzing corresponding blanks (untreated cells).

When developing a reliable quantitative analysis of  $^{15}\text{N}$ -nitrite, there is a clear risk of interference between  $^{15}\text{N}$ -NAT and  $^{14}\text{N}$ -NAT containing one  $^{13}\text{C}$  atom (due to its natural abundance of 1.1%). Chao *et al*<sup>24</sup> showed a 2.2%-interference due to  $^{13}\text{C}$ , which was in good agreement with what is theoretically expected. We did not observe any interference when the quantification was performed using fresh reactants and culture medium. Thus, a LOQ of 1 nM was obtained LC-ITMS/MS which is comparable to the LOQ obtained by Axton *et al.* on their Q-Trap<sup>25</sup>. However, ambient nitrogen oxides (NO<sub>x</sub>) are rapidly able to dissolve into them, leading to an interference in the experimental blanks (Figure 5). This interference was estimated to be around 50 to 60 nM in  $^{14}\text{NO}_x$  (using the transition  $m/z$  170 to 156), which is equivalent to the signal of 1 nM of  $^{15}\text{N}$ -NAT for the corresponding transition ( $m/z$  171 to

156). Consequently, the working LOQ was set at 5 nM for the validation step, taking in account the signal-over-blank ratio rather than the signal-over-noise one.

Nevertheless, this concentration level is satisfactory enough for the accurate quantification of nitrites in the real samples.

### **Method validation**

The next step of this study was the investigation of the linearity range, reproducibility, accuracy, precision, interferences, percent recovery, and carryover of the developed LC-ITMS/MS method.

The linearity range and the LOQ were determined from 3 standard curves of nitrite ions. The LOQ was limited to 5 nM, as described in the previous section. The calibration curve of  $^{15}\text{N}$ -NAT adduct was linear between 5 and 200 nM for  $\text{Na}^{15}\text{NO}_2$  and  $\text{GS}^{15}\text{NO}$  and between 250 and 5000 nM for  $\text{Na}^{15}\text{NO}_3$ , with the coefficient of determination ( $r^2$ ) higher than 0.9956. The intra- and inter-day variabilities of the method were evaluated by using quality control samples and the results are summarized in Table 2. Three concentrations of  $\text{Na}^{15}\text{NO}_2$  and  $\text{GS}^{15}\text{NO}$  (15, 50, 180 nM), and of  $\text{Na}^{15}\text{NO}_3$  (300, 2500, 4000 nM) were spiked into HBSS ( $n = 6$ ), and the concentration was calculated by using a six-point calibration curve for  $\text{Na}^{15}\text{NO}_2$  and  $\text{GS}^{15}\text{NO}$  (5, 10, 20, 50, 100, 200 nM), and for  $\text{Na}^{15}\text{NO}_3$  (250, 500, 1250, 2500, 5000 nM). The accuracy was determined as the deviation (%) of the calculated concentrations from the nominal concentrations. The precision was determined as the relative standard deviation (RSD) of the six measurements. Satisfactory accuracies were obtained with intra- and inter-day bias lower than 5.2 % and 5.3 % for  $\text{Na}^{15}\text{NO}_2$ , 1.9 % and 6.7 % for  $\text{GS}^{15}\text{NO}$ , and 7.7 % and 9.4 % for  $\text{Na}^{15}\text{NO}_3$ , respectively, over the studied concentration ranges. The intra- and inter-day precision ranged from 3.0 to 7.1 % for  $\text{Na}^{15}\text{NO}_2$ , from 7.7 to 13.4 % for  $\text{GS}^{15}\text{NO}$  and from 5.6 to 8.7 % for  $\text{Na}^{15}\text{NO}_3$  in HBSS. These ranges were within the criteria stated in the FDA guidance on bioanalytical method validation (Table 2).

Additionally, the product NAT was found stable after storage at -80 °C for 3 months and freezing/thaw for 2 cycles (data not shown).

### **Intestinal permeability of GS<sup>15</sup>NO *in vitro***

To evaluate the intestinal permeability of nitrate, nitrite and RSNOs, we needed to determine their concentration in the apical and basolateral compartments after incubation (Figure 6). To the best of our knowledge, for the first time, one single derivatization technique is used to determine the three considered analytes. In our approach, all GSNO metabolites, nitrites, nitrates and RSNOs, were derivatized to the same compound (NAT) and then quantified by LC-ITMS/MS. Free nitrites were measured first. The nitrate concentration was then determined after enzymatic reduction of nitrate ions subtracting the concentration of free nitrites. Similarly, RSNOs concentrations are calculated by subtracting the concentration of free nitrites from the sum “RSNOs + nitrites” measured after the S-NO bond cleavage with mercuric ions. In the apical compartment, the decomposition of GSNO into nitrites and nitrates was also checked by direct HPLC-UV as proposed by Parent *et al* for concentrations in the micromolar range<sup>30</sup>. GSNO was found to be stable under the present operating conditions (data not shown). Nevertheless, in the basolateral compartment, GSNO degradation could not be investigated by HPLC-UV because of the very low measured concentrations (nanomolar range). In this compartment, the transfer of the NO moiety of GSNO on cysteine residues of peptides and proteins is possible, resulting in a formation of other RSNOs. That is the reason why, in the basolateral compartment, it is preferable to use the term RSNOs rather than GSNO to take into account all possible compounds reacting with mercuric ions. Nevertheless, whatever the GS<sup>15</sup>NO fate in the basolateral compartment, it is clear that the <sup>15</sup>N-labeled species analyzed by our LC-ITMS/MS method originates from this drug.

The TEER values measured before and after 1 h of GS<sup>15</sup>NO permeation through the Caco-2 cell monolayer was higher than 500 Ω·cm<sup>-2</sup>. Meanwhile, the permeability percentage of the sodium fluorescein was less than 5 %. These results indicated a confluent and unaltered monolayer.

In the Biopharmaceutics Classification System<sup>31</sup>, drugs are assigned within four classes depending on their aqueous solubility and intestinal permeability. Three classes of intestinal permeability are defined according to drug  $P_{app}$  value: high permeability compounds such as propranolol show  $P_{app}$  value higher than  $10^{-5} \text{ cm}\cdot\text{s}^{-1}$ , while low permeability compounds such as furosemide show  $P_{app}$  value less than  $1\cdot 10^{-6} \text{ cm}\cdot\text{s}^{-1}$ <sup>32</sup>. Intermediate values correspond to “middle permeability” drugs. It was found that <sup>15</sup>N-nitrite has a  $P_{app}$  value in the range of  $(0.32 - 0.47)\times 10^{-6} \text{ cm}\cdot\text{s}^{-1}$ , RS<sup>15</sup>NOs in the range of  $(0.16 - 0.35)\times 10^{-6} \text{ cm}\cdot\text{s}^{-1}$ , while <sup>15</sup>N-nitrate is in the range of  $(1.65 - 1.79)\times 10^{-6} \text{ cm}\cdot\text{s}^{-1}$ , which demonstrated that GS<sup>15</sup>NO belongs to the class of middle permeability compounds. In addition, GSNO showed concentration-dependent distribution in both compartments in the tested concentration range (10-100  $\mu\text{M}$ ) (Figure 6), and concentration-independent permeability. Noteworthy, the present LC/ITMS/MS method allows us to reach the low concentrations of NO-related species in the basolateral compartment, even at the lowest dose of GSNO applied to the cellular barrier model (10  $\mu\text{M}$ ). Applying fluorescence with the same derivatization process (DAN) limits the permeability studies to the highest concentration of GSNO (100  $\mu\text{M}$ ). High levels of NO species (nitrite, nitrate and RSNOs) in the blank demonstrate the necessity of using isotope labeling to improve the method LOQ, and sample dilution contributes to a lower risk of matrix interference.

## CONCLUSIONS

We have developed and validated a LC-ITMS/MS method capable of selectively monitoring NO species metabolized from <sup>15</sup>N labeled GSNO as NAT adducts using an Ion Trap Mass Spectrometer. Compared with other published approaches, this method combines several original features such as (i) the use of a single derivatization technique for the three considered analytes (nitrites, nitrates and RSNOs), (ii) a new described fragmentation pattern that is at least as sensitive as (sometime even more sensitive than) the previously described methods (in the nM range)<sup>24,25,26</sup> on triple quadrupole mass spectrometers, and (iii) the first report of a <sup>15</sup>N labeling method applied to an intestinal barrier model.

The IT mass spectrometer enables us to reach a very satisfying sensitivity thanks to an original “indirect” MS/MS transition ( $m/z$  171 to 156 via an acetonitrile adduct  $m/z$  212 formation) obtained in Higher-energy Collision Dissociation with a limit of quantification of 1 nM on  $^{15}\text{NO}$  freed from  $\text{GS}^{15}\text{NO}$ . The working LOQ was set at 5 nM to overcome interferences produced by  $^{14}\text{NO}$  present in the real samples. The assay, applied to the study of the intestinal permeability of  $\text{GS}^{15}\text{NO}$  with an *in vitro* model of this physiological barrier, classifies the S-nitrosoglutathione in the middle permeability class according to FDA guidelines.

The work was the preamble of future assays of NO species metabolized from labeled  $\text{GS}^{15}\text{NO}$  or other NO donors in the cells or tissues. It also opens the perspective of a more fundamental work such as the study of the reactivity of the ion  $[\text{NAT}+\text{H}]^+$  in HCD tandem mass spectrometry in the presence of acetonitrile.

Furthermore, the use of *in vitro* models of intestinal permeability is of key importance to evaluate the drug (GSNO) bioavailability after oral administration. To the best of our knowledge, this work provides the first report of a  $^{15}\text{N}$ -labeled drug using an intestinal permeability model. In the future, the transposition of our approach to other biological matrices (plasma, tissues, organs like aorta) using sample preparation protocols already described<sup>33,34</sup> constitutes a natural extension of the fields of application.

### **Acknowledgements**

Authors are grateful to the program of China Scholarship Council for the financial support of Ms Haiyan Yu's PhD thesis (grant NO. 201506270166). Authors also thank Dr Philippe Giummelly (CITHEFOR, Université de Lorraine) for the synthesis of  $\text{GS}^{15}\text{NO}$ .

### **REFERENCES**

- 1 Moncada S, Palmer RM, Higgs EA. Nitric oxide: physiology, pathophysiology, and pharmacology. *Pharmacol Rev.* 1991;43(2):109–142.

- 2 Cooke JP, Dzau VJ. Nitric oxide synthase: Role in the genesis of vascular disease. *Annu Rev Med.* 1997;48:489–509.
- 3 Vallance P, Leone A, Calver A, Collier J, Moncada S. Accumulation of an Endogenous Inhibitor of Nitric-Oxide Synthesis in Chronic-Renal-Failure. *Lancet.* 1992;339(8793):572–575.
- 4 Lundberg JO, Weitzberg E, Gladwin MT. The nitrate-nitrite-nitric oxide pathway in physiology and therapeutics. *Nat Rev Drug Discov.* 2008;7(2):156–167. Doi: 10.1038/nrd2466.
- 5 Loo B, Labugger R, Skepper JN, et al. Enhanced Peroxynitrite Formation Is Associated with Vascular Aging. *J Exp Med.* 2000;192(12):1731–1744. Doi: 10.1084/jem.192.12.1731.
- 6 Münzel T, Steven S, Daiber A. Organic nitrates: Update on mechanisms underlying vasodilation, tolerance and endothelial dysfunction. *Vascul Pharmacol.* 2014;63(3):105–113. Doi: 10.1016/j.vph.2014.09.002.
- 7 Csont T, Ferdinandy P. Cardioprotective effects of glyceryl trinitrate: beyond vascular nitrate tolerance. *Pharmacol Ther.* 2005;105(1):57–68. Doi: 10.1016/j.pharmthera.2004.10.001.
- 8 Broniowska KA, Diers AR, Hogg N. S-Nitrosoglutathione. *Biochim Biophys Acta. BBA - Gen Subj.* 2013;1830(5):3173–3181. Doi: 10.1016/j.bbagen.2013.02.004.
- 9 Gaucher C, Boudier A, Dahboul F, Parent M, Leroy P. S-nitrosation/Denitrosation in Cardiovascular Pathologies: Facts and Concepts for the Rational Design of S-nitrosothiols. *Curr Pharm Des.* 2013;19(3):458–472.
- 10 Wu W, Perrin-Sarrado C, Ming H, et al. Polymer nanocomposites enhance S-nitrosoglutathione intestinal absorption and promote the formation of releasable nitric oxide stores in rat aorta. *Nanomedicine-Nanotechnol Biol Med.* 2016;12(7):1795–1803. Doi: 10.1016/j.nano.2016.05.006.
- 11 Chan OH, Stewart BH. Physicochemical and drug-delivery considerations for oral drug bioavailability. *Drug Discov Today.* 1996;1(11):461–473.

- 12 Badhan R, Penny J, Galetin A, Houston IB. Methodology for Development of a Physiological Model Incorporating CYP3A and P-Glycoprotein for the Prediction of Intestinal Drug Absorption. *J Pharm Sci*. 2009;98(6):2180–2197. Doi: 10.1002/jps.21572.
- 13 Artursson P. Cell-Cultures as Models for Drug Absorption Across the Intestinal-Mucosa. *Crit Rev Ther Drug Carrier Syst*. 1991;8(4):305–330.
- 14 Alqahtani S, Mohamed LA, Kaddoumi A. Experimental models for predicting drug absorption and metabolism. *Expert Opin Drug Metab Toxicol*. 2013;9(10):1241–1254. Doi: 10.1517/17425255.2013.802772.
- 15 Miersch S, Mutus B. Protein S-nitrosation: Biochemistry and characterization of protein thiol–NO interactions as cellular signals. *Clin Biochem*. 2005;38(9):777–791. Doi: 10.1016/j.clinbiochem.2005.05.014.
- 16 Bryan NS, Grisham MB. Methods to detect nitric oxide and its metabolites in biological samples. *Free Radic Biol Med*. 2007;43(5):645–657. Doi: 10.1016/j.freeradbiomed.2007.04.026.
- 17 Marzinzig M, Nussler AK, Stadler J, et al. Improved Methods to Measure End Products of Nitric Oxide in Biological Fluids: Nitrite, Nitrate, and S-Nitrosothiols. *Nitric Oxide*. 1997;1(2):177–189. Doi: 10.1006/niox.1997.0116.
- 18 Tsikas D. Methods of quantitative analysis of the nitric oxide metabolites nitrite and nitrate in human biological fluids. *Free Radic Res*. 2005;39(8):797–815. Doi: 10.1080/10715760500053651.
- 19 Schmidt TC, Zwank L, Elsner M, Berg M, Meckenstock RU, Haderlein SB. Compound-specific stable isotope analysis of organic contaminants in natural environments: a critical review of the state of the art, prospects, and future challenges. *Anal Bioanal Chem*. 2004;378(2):283–300. Doi: 10.1007/s00216-003-2350-y.
- 20 Tsikas D. Pentafluorobenzyl bromide—A versatile derivatization agent in chromatography and mass spectrometry: I. Analysis of inorganic anions and organophosphates. *J Chromatogr B*. 2017;1043:187–201. Doi: 10.1016/j.jchromb.2016.08.015.

- 21 Hanff E, Boehmer A, Jordan J, Tsikas D. Stable-isotope dilution LC-MS/MS measurement of nitrite in human plasma after its conversion to S-nitrosoglutathione. *J Chromatogr B-Anal Technol Biomed Life Sci.* 2014;970:44–52. Doi: 10.1016/j.jchromb.2014.08.041.
- 22 Li H, Meininger CJ, Wu G. Rapid determination of nitrite by reversed-phase high-performance liquid chromatography with fluorescence detection. *J Chromatogr B Biomed Sci App.* 2000;746(2):199–207. Doi: 10.1016/S0378-4347(00)00328-5.
- 23 Marzinzig M, Nussler AK, Stadler J, et al. Improved methods to measure end products of nitric oxide in biological fluids: Nitrite, nitrate, and S-nitrosothiols. *Nitric Oxide-Biol Chem.* 1997;1(2):177–189. Doi: 10.1006/niox.1997.0116.
- 24 Chao MR, Shih YM, Hsu YW, et al. Urinary nitrite/nitrate ratio measured by isotope-dilution LC–MS/MS as a tool to screen for urinary tract infections. *Free Radic Biol Med.* 2016;93:77–83. Doi: 10.1016/j.freeradbiomed.2016.01.025.
- 25 Axton ER, Hardardt EA, Stevens JF. Stable isotope-assisted LC–MS/MS monitoring of glyceryl trinitrate bioactivation in a cell culture model of nitrate tolerance. *J Chromatogr B.* 2016;1019:156–163. Doi: 10.1016/j.jchromb.2015.12.010.
- 26 Shin S, Fung HL. Evaluation of an LC–MS/MS assay for <sup>15</sup>N-nitrite for cellular studies of l-arginine action. *J Pharm Biomed Anal.* 2011;56(5):1127–1131. Doi: 10.1016/j.jpba.2011.08.017.
- 27 Saville B. A scheme for the colorimetric determination of microgram amounts of thiols. *Analyst.* 1958;83(993):670–2. Doi: 10.1039/AN9588300670.
- 28 Parent M, Dahboul F, Schneider R, et al. A Complete Physicochemical Identity Card of S-nitrosoglutathione. *Curr Pharm Anal.* 2013;9(1):31–42.
- 29 Jobgen WS, Jobgen SC, Li H, Meininger CJ, Wu G. Analysis of nitrite and nitrate in biological samples using high-performance liquid chromatography. *J Chromatogr B.* 2007;851(1-2):71–82. Doi: 10.1016/j.jchromb.2006.07.018.
- 30 Parent M, Dahboul F, Schneider R, Clarot C, Maincent P, Leroy P, Boudier A. A Complete Physicochemical Identity Card of S-Nitrosoglutathione. *Current Pharmaceutical Analysis.* 2013;9:31–42.

- 31 U.S. Department of Health and Human Services Food and Drug Administration Center for Drug Evaluation and Research (CDER). Waiver of in vivo bioavailability and bioequivalence studies for immediate-release solid oral dosage forms based on a biopharmaceutics classification system. *Biopharmaceutics*. 2015.
- 32 Peng Y, Yadava P, Heikkinen AT, Parrott N, Railkar A. Applications of a 7-day Caco-2 cell model in drug discovery and development. *Eur J Pharm Sci*. 2014;56:120–130. Doi: 10.1016/j.ejps.2014.02.008.
- 33 Warnecke A, Luessen P, Sandmann J, et al. Application of a stable-isotope dilution technique to study the pharmacokinetics of human N-15-labelled S-nitrosoalbumin in the rat: Possible mechanistic and biological implications. *J Chromatogr B-Anal Technol Biomed Life Sci*. 2009;877(13):1375–1387. Doi: 10.1016/j.jchromb.2008.11.035.
- 34 Damacena-Angelis C, Oliveira-Paula GH, Pinheiro LC, et al. Nitrate decreases xanthine oxidoreductase-mediated nitrite reductase activity and attenuates vascular and blood pressure responses to nitrite. *Redox Biol*. 2017;12:291–299. Doi: 10.1016/j.redox.2017.03.003.

Table 1: Ion composition of the MS/MS spectra of the  $^{14}\text{N}$ -NAT or  $^{15}\text{N}$ -NAT adduct in CID (35 eV) and HCD (50 eV) depending on the organic modifier composing the chromatographic mobile phase (solvent S). The NAT adduct was infused in a mixture of a 10 mM-acetic acid aqueous solution containing 40% of the solvent S. The relative abundance (%) of each ion is indicated in parentheses. Nd: not detected

Labeling	MS/MS	Solv. S <sup>a</sup>	Observed $m/z$ for $[\text{NAT}+\text{H}]^+$ precursor ion					
			$[\text{NAT}+\text{H}]^+$	$[\text{NAT}-\text{N}_2+\text{H}]^+$	$[\text{C}_9\text{H}_7]^{\text{+b}}$	$[\text{NAT}+\text{H}+\text{S}]^+$	$[\text{NAT}-\text{N}_2+\text{H}+\text{S}]^+$	$[\text{NAT}-\text{N}_2-\text{HCN}+\text{H}+\text{S}]^+$
$^{14}\text{N}$ -NAT	CID (35eV)	MeOH	170 <sub>(38)</sub>	142 <sub>(19)</sub>	115 <sub>(100)</sub>	Nd	Nd	Nd
		ACN	170 <sub>(36)</sub>	142 <sub>(18)</sub>	115 <sub>(100)</sub>	Nd	Nd	Nd
	HCD (50eV)	ACN	170 <sub>(46)</sub>	Nd	115 <sub>(100)</sub>	211 <sub>(0.1)</sub>	183 <sub>(1.1)</sub>	156 <sub>(46)</sub>
		d <sub>3</sub> -ACN	170 <sub>(45)</sub>	Nd	115 <sub>(100)</sub>	214 <sub>(0.1)</sub>	186 <sub>(1.1)</sub>	159 <sub>(45)</sub>
$^{15}\text{N}$ -NAT	CID (35eV)	MeOH	171 <sub>(38)</sub>	142 <sub>(19)<sup>c</sup></sub>	115 <sub>(100)</sub>	Nd	Nd	Nd
		ACN	171 <sub>(36)</sub>	142 <sub>(15)<sup>c</sup></sub>	115 <sub>(100)</sub>	Nd	Nd	Nd
	HCD (50eV)	ACN	171 <sub>(45)</sub>	Nd	115 <sub>(100)</sub>	212 <sub>(0.1)</sub>	183 <sub>(1.1)<sup>c</sup></sub>	156 <sub>(40)<sup>c</sup></sub>
		d <sub>3</sub> -ACN	171 <sub>(46)</sub>	Nd	115 <sub>(100)</sub>	215 <sub>(0.2)</sub>	186 <sub>(1.0)<sup>c</sup></sub>	159 <sub>(42)<sup>c</sup></sub>

Remarks: a: The NAT adduct is infused in a mixture of a 10 mM-acetic acid aqueous solution containing 40% of solvent S (MeOH, ACN or d<sub>3</sub>-ACN)  
b: This ion is also corresponding to  $[\text{NAT}-\text{N}_2-\text{HCN}+\text{H}]^+$  (see also Axton *et al*<sup>25</sup> and also Shin *et al*<sup>26</sup>)  
c: For these ions, the loss is 29 u because N<sub>2</sub> is containing the labeled nitrogen ( $^{15}\text{N}$ ).

Table 2. Inter-day and intra-day variability of quality control samples for  $^{15}\text{N}$ -nitrite *S*-nitrosoglutathione ( $\text{GS}^{15}\text{NO}$ ) and  $^{15}\text{N}$ -nitrate analysis with IS.  $^{15}\text{N}$ -nitrite,  $\text{GS}^{15}\text{NO}$  and  $^{15}\text{N}$ -nitrate were spiked into HBSS buffer ( $n = 6$ ), and the concentration was calculated by using related six-point calibration curve (5, 10, 20, 50, 100, 200 nM) of  $^{15}\text{N}$ -nitrite and *S*-nitrosoglutathione ( $\text{GS}^{15}\text{NO}$ ), and five-point calibration curve (250, 500, 1250, 2500, 5000 nM) of  $^{15}\text{N}$ -nitrate. Accuracy was determined as the deviation (%) of calculated concentrations from the nominal concentrations. Precision was determined as the relative standard deviation (RSD) of the 6 measurements.

NO species	Concentration (nM)	Intra-day		Inter-day	
		Accuracy (%)	Precision (%)	Accuracy (%)	Precision (%)
$^{15}\text{N}$ -nitrite	15	105.2±6.4	6.1	104.7±7.0	6.7
	50	99.0±6.8	6.9	94.7±2.8	3.0
	180	98.6±5.3	5.4	102.7±7.3	7.1
$\text{GS}^{15}\text{NO}$	15	98.1±13.1	13.4	93.3±11.8	12.6
	50	99.1±10.9	11.0	96.0±7.4	7.7
	180	100.0±12.7	12.7	101.5±11.4	11.3
$^{15}\text{N}$ -nitrate	300	103.0±6.9	6.7	103.0±7.0	6.8
	2500	100.8±5.6	5.6	100.6±8.7	8.7
	4000	107.7±8.5	7.9	109.4±8.8	8.1

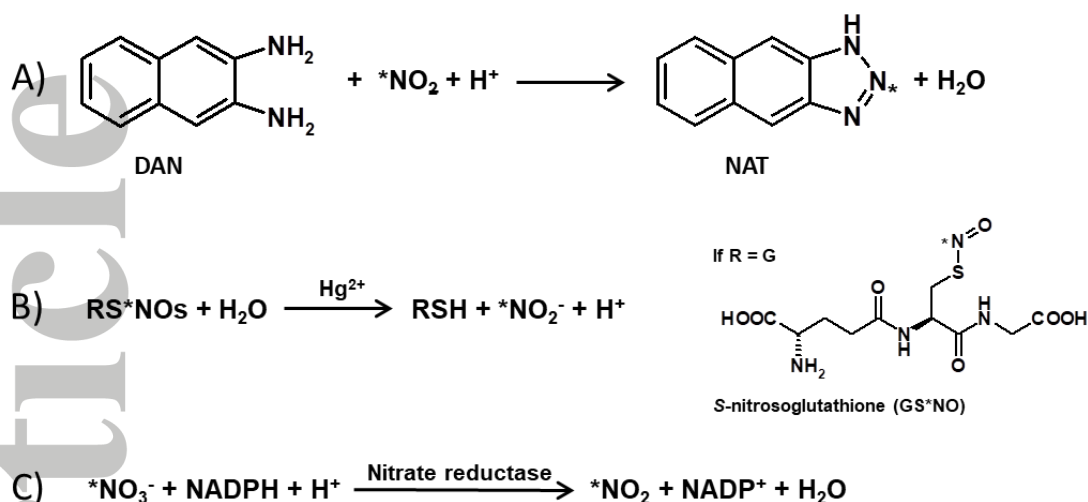


Figure 1. Principal reactions involved in this study. A) Derivatization of nitrite ion with 2,3-diaminonaphthalene (DAN) leading to a 2,3-naphthotriazole (NAT) derivative. The nitrogen transferred from the nitrite ion is indicated with an asterisk (\*); B) Release of nitrites from the S-nitrosoglutathione (GSNO) catalyzed by mercuric ions and C) Reaction of nitrate conversion into nitrite ion catalyzed by a nitrate reductase in presence of cofactor (here NADPH = nicotinamide adenine dinucleotide phosphate).

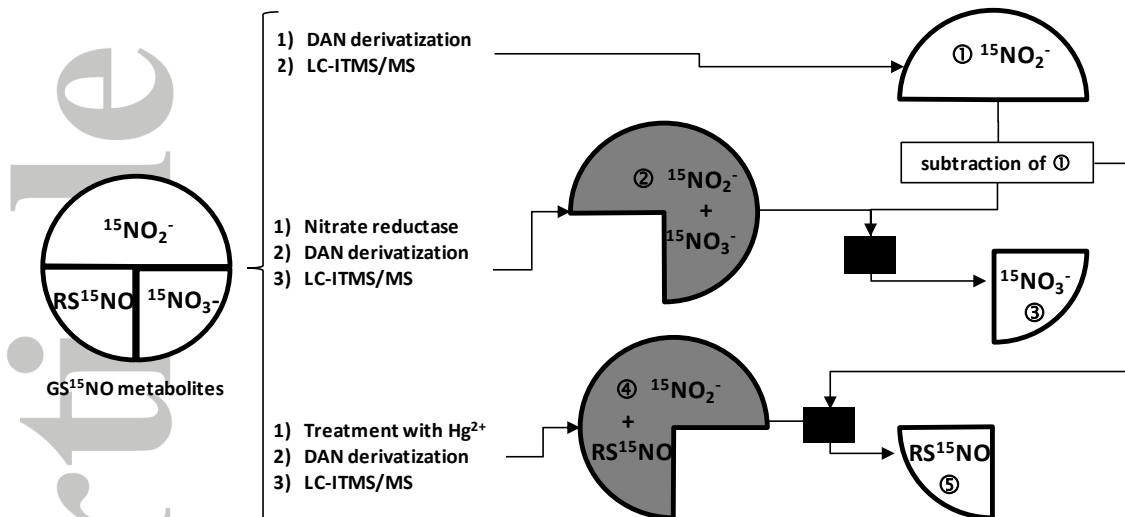


Figure 2. Strategy of analysis of the different  $GS^{15}NO$  metabolites obtained during the *in vitro* study using the same LC-ITMS/MS approach. The concentration of free  $^{15}N$ -nitrites ① after incubation is directly obtained after DAN derivatization followed by LC-ITMS/MS. Free  $^{15}N$ -nitrates are obtained after enzymatic (nitrate reductase) pretreatment of the metabolite pool. The quantification by LC-MS/MS after DAN derivatization of this sample provides the cumulative concentration ② of free  $^{15}N$ -nitrites +  $^{15}N$ -nitrates (reduced into nitrites). The concentration in free  $^{15}N$ -nitrates ③ is deduced from result ② by subtracting the concentration of free  $^{15}N$ -nitrites ①. The concentration of  $RS^{15}NO$ s is obtained after the pretreatment of the metabolite pool with  $Hg^{2+}$ . The quantification by LC-MS/MS after DAN derivatization of this sample provides the cumulative concentration ④ of free  $^{15}N$ -nitrites +  $GS^{15}NO$  (converted into nitrites, see reaction 2 in figure 1). The concentration of  $RS^{15}NO$  ⑤ is deduced from result ④ by subtracting the concentration of free  $^{15}N$ -nitrites ①.

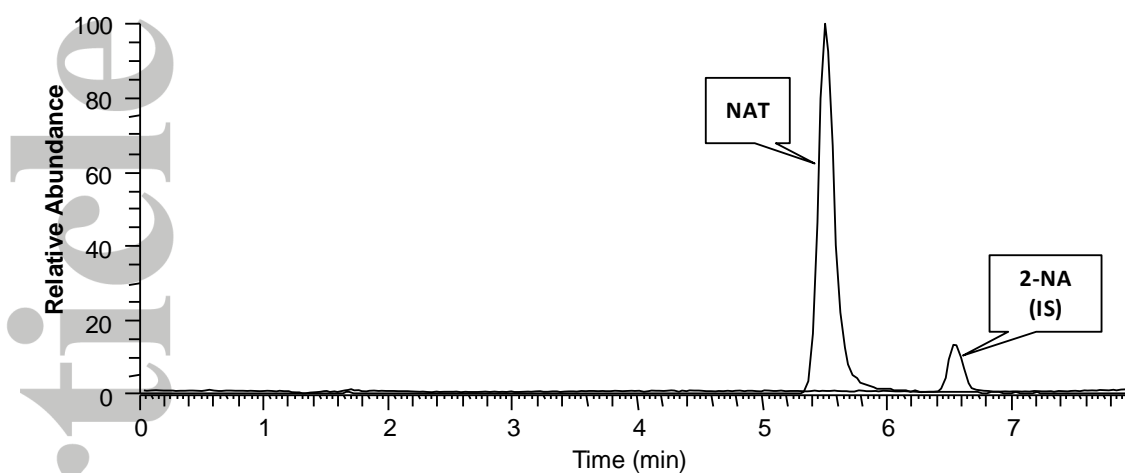


Figure 3. Representative LC-ESI-ITMS/MS chromatogram (conditions given in the experimental section) of the 2,3-naphthotriazole (NAT) derivative and the internal standard (IS, 2-naphthylamine (2-NA)).

Accepted Article

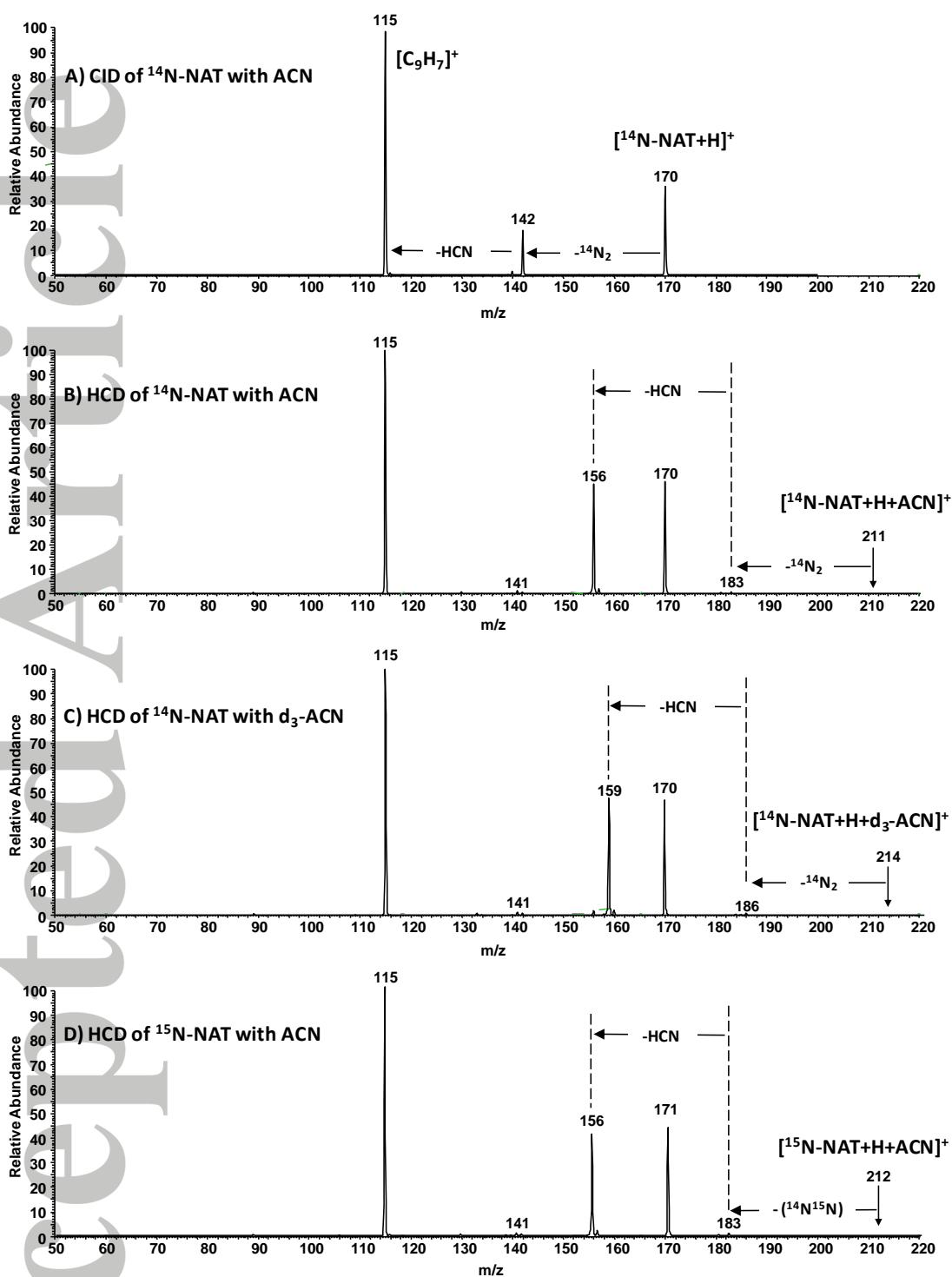


Figure 4. Fragmentation of the protonated molecular ion of NAT diluted at  $2 \mu\text{M}$  in the chromatographic mobile phase. A) CID at 35 eV of  $[\text{}^{14}\text{N-NAT+H}]^+$  ( $m/z$  170) using acetonitrile (ACN), B) HCD at 50 eV of  $[\text{}^{14}\text{N-NAT+H}]^+$  using ACN, C) HCD at 50 eV of  $[\text{}^{14}\text{N-NAT+H}]^+$  using deuterated acetonitrile ( $\text{d}_3\text{-ACN}$ ) and D) HCD at 50 eV of  $[\text{}^{15}\text{N-NAT+H}]^+$  ( $m/z$  171) using ACN. See also Table 1 for complementary information.

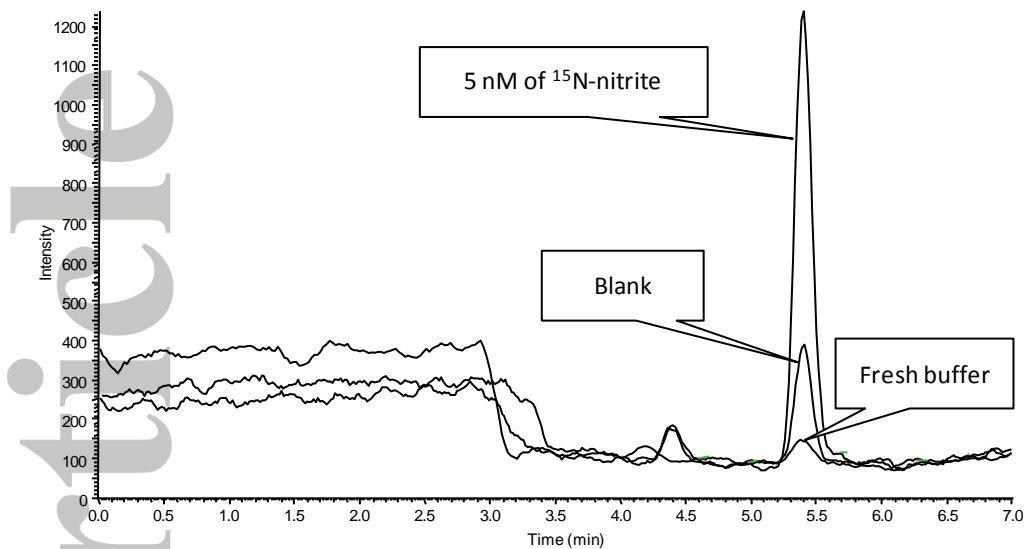
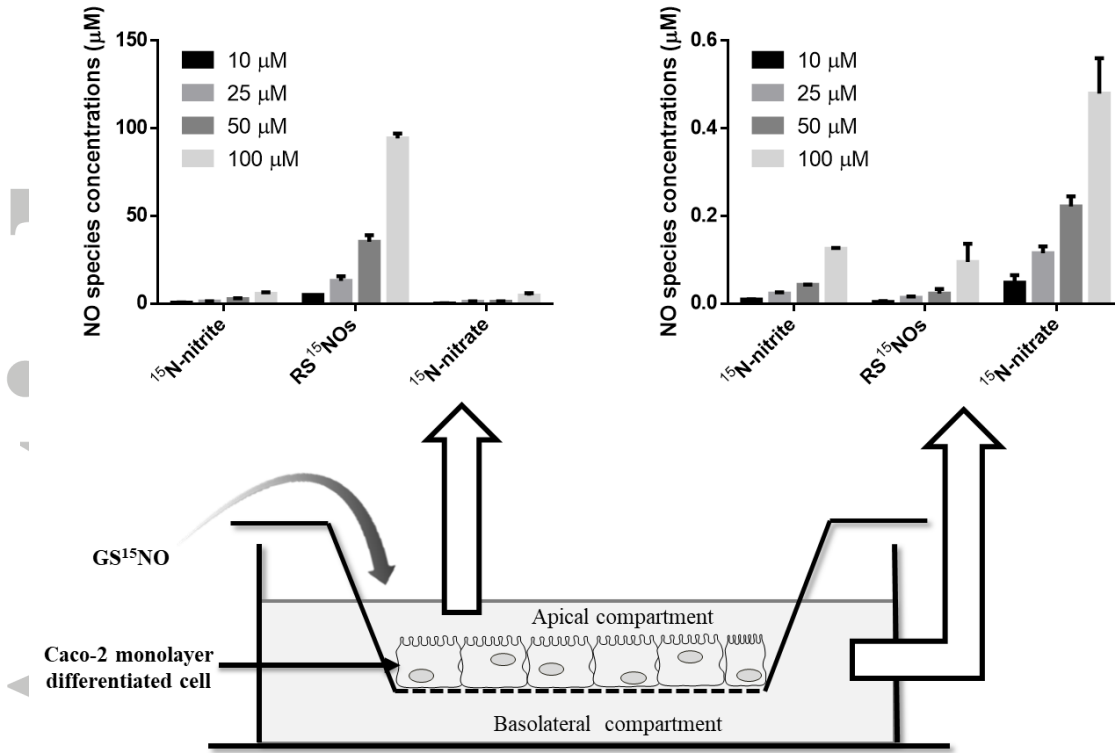


Figure 5. Representative ion chromatograms under selected reaction monitoring (SRM) transition of  $m/z$  171  $\rightarrow$  156, corresponding to derivatization of 5 nM  $^{15}\text{N}$ -nitrite in HBSS buffer, blank of the *in vitro* study and freshly prepared HBSS buffer.

Accepted Article



Figure

6. Permeation of 10, 25, 50 or 100 μM of  $^{15}\text{N}$  labeled *S*-nitrosoglutathione (GS $^{15}\text{NO}$ ) through an *in vitro* model of intestinal barrier (differentiated Caco-2 cell monolayer) during 1 h at 37 °C. GS $^{15}\text{NO}$  metabolites (nitric oxide (NO) species concentrations) were quantified in both compartments, n = 3. Results are expressed as mean ± SD.

Accepted